Journal of Hydrology 404 (2011) 67–76

Contents lists available at ScienceDirect

Journal of Hydrology

journal homepage: www.elsevier.com/locate/jhydrol

Precipitation variability in Northeast China from 1961 to 2008

Liqiao Liang [a], Lijuan Li [a,*], Qiang Liu [b]

[a] Institute of Geographic Sciences and Natural Resources Research, CAS, No. 11A, Datun Road, Chaoyang District, Beijing 100101, China
[b] School of Environment, Beijing Normal University, No. 19, Xinwai Street, Haidian District, Beijing 100875, China

ARTICLE INFO

Article history:
Received 17 October 2010
Received in revised form 30 March 2011
Accepted 8 April 2011
Available online 16 April 2011
This manuscript was handled by A. Bardossy, Editor-in-Chief, with the assistance of Efrat Morin, Associate Editor

Keywords:
Precipitation
Spatial distribution
Trend
Climate jump
Periodicity
Northeast China

SUMMARY

Variability in precipitation plays an important role in the way it influences ecological and agricultural water requirements. This is especially true for semi-humid and semi-arid regions exemplified in certain regions in Northeast China. The temporal variation and spatial distribution of precipitation in Northeast China from 1961 to 2008 was investigated in this study by means of a linear fitted model, the Mann–Kendall test, the moving *t*-test, and the Morlet wavelet and Kriging (exponential) interpolation methods. Results indicate that: (a) the monthly precipitation rate varied considerably wherein summer precipitation accounted for 65.7% of the annual total value; (b) a decreasing trend in precipitation was found in the data obtained from 77 (annual) and 80 (summer) of the 98 meteorological stations throughout a 48 year period (from 1961 to 2008) while climate jumps were detected in 77% (annual) and 67% (summer); (c) three climate jumps and periods of 2.3 and 3.3 years (significant at a 95% confidence level) were detected on a regional scale; (d) the mean annual and summer precipitation rates decreased in a southeastern to northwestern trajectory throughout the 48 year period due both to the influence of the East Asian monsoon and to topography. All these findings can help provide rational regulatory and managerial policy in relation to water resources to maintain the health of the various ecosystems that make up Northeast China.

1. Introduction

Changes in climate may have already affected elements of the hydrologic cycle such as precipitation redistribution, snow accumulation and meltwater, evapotranspiration, and the surface and subsurface water table (IPCC, 1995). Land area precipitation generally increased throughout the twentieth century between latitude 30°N and 85°N, but notable decreases have also occurred in the past 30–40 years from latitude 10°S to 30°N (IPCC, 2007). Asia experienced multiple disaster events in 2010 due to changes in precipitation such as the spring drought that occurred in Southwest China as well as floods that occurred in Pakistan, India, and many provinces in China. Precipitation is regarded as the primary source of water resource in China and, therefore, most water resource projects are designed and implemented based on the historical pattern of water availability, quality, and demand, assuming a constant climatic order of behavior (Westmacott and Burn, 1997; Abdul Aziz and Burn, 2006; Liu et al., 2008). Appropriate adaptation strategies can be implemented to investigate present and probable future climate change patterns and their impacts on water resources. Precipitation is one of the most important variables in diagnosing climate change as well as revealing the eco-environmental response to climate change on a regional scale (Cannarozzo et al., 2006). Both temporal and spatial patterns of precipitation and evapotranspiration influence eco-hydrological processes (Oguntunde et al., 2006; Cannarozzo et al., 2006; McVicar et al., 2007) and, consequently, regional economies strongly tied to agriculture and raising livestock (O'Neal et al., 2002; Wei et al., 2005; Guo et al., 2006). Therefore, a better understanding of precipitation variability on a regional scale will assist in determining water management policies. It will also help in planning sustainable agricultural practices that will contribute to ecological conservation and environmental protection.

The objectives of this study were: (i) to explore variability in precipitation on both monthly and annual timescales; (ii) to detect climate jumps and periodicity in precipitation throughout a 48 year climatological period from 1961 to 2008; and (iii) to investigate the spatial distribution of precipitation in Northeast China.

2. Study area

Northeast China (from lat 38°40′ to lat 53°34′N and from long 115°05′ to long 135°02′E) is a geographical region of China (Fig. 1). Its total area is 1.24×10^6 km^2 and supports a population of 119.0×10^6 as established by the 2003 census (Liu, 2007). The landscape can be characterized by plains separated by three major mountain systems: the Greater Khingan Range, Lesser Khingan

* Corresponding author. Tel./fax: +86 10 64889309.
E-mail address: lilj@igsnrr.ac.cn (L. Li).

0022-1694/$ - see front matter © 2011 Elsevier B.V. All rights reserved.
doi:10.1016/j.jhydrol.2011.04.020

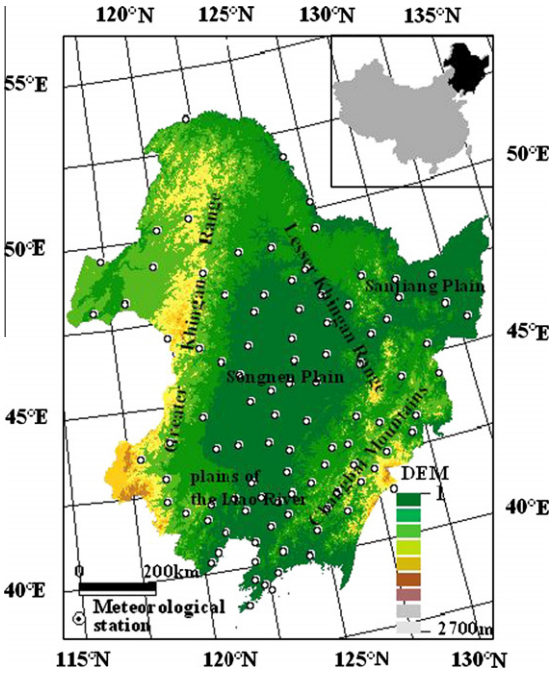

Fig. 1. The location of Northeast China (black shading) and Mainland China (light shading) are provided in the inset map. The map base provides the locations of the meteorological stations (dots) in the study area.

Range, and the Changbai Mountains. Northeast China is under the sway of a monsoon system that characterizes the medium latitudinal zone of China where climate alters from warm temperate, temperate, to cool temperate and the longitudinal zone where climate alters from humid, semi humid, to semi-arid. Long-term annual air temperature varies spatially from −4.7 °C to 10.7 °C, and annual range of air temperature can reach up to 40 °C. The length of time for which snow covers the ground can last as long as half a year in certain regions (Zhang et al., 2006).

Arable land accounts for 29.77% of all land area in Northeast China. In terms of area, paddy fields outnumber dry land by a factor of seven. The proportion of arable land is greater than 55% in the Songnen Plain and the plains of the Liao River (Zhang et al., 2006). The plains of the Liao River, the Songnen Plain, and the Sanjiang Plain, that together produce more than 40% of the grain output produced in the entire country (Yin et al., 2006), are important agricultural regions in China and, consequently, must be taken into account when discussing the safety of the national food supply. In April, 2009, the National Development and Reform Commission (NDRC) launched the "Plan for Increasing the National Grain Production Capacity by 50 Billion Kilograms (2009–2020)," and planed to increase grain production capacity by 5 billion kg in Northeast China. However, global change and intensified human exploitation of land and water resources in the last five decades have altered the hydrological cycle and added to water scarcity and the spatial–temporal variation of the resource (Ni and Zhang, 2000; Jiang et al., 2009; Liang et al., 2010). Several water-based and eco-environmental problems have risen to prominence in recent years such as the decreasing groundwater table in plains systems, an overall reduction of wetland area, black soil erosion, degradation of grassland, desertification, an increase in soil salinization, etc. (Liu, 2007). Water resource problems, especially in relation to water scarcity, have become one of the most important factors that influence the health of an ecosystem and one of the primary factors that threaten agriculture in the Northeast China.

3. Data and methods

3.1. Data description

For this study, monthly precipitation data from the China Meteorological Administration (CMA) were gathered from 98 meteorological stations located throughout Northeast China during a period from January, 1961, to December, 2008. Fig. 1 provides the locations of these meteorological stations. Monthly data were derived from daily data, and the annual data were derived from the monthly data. The 48-year period investigated was considered long enough to ascertain reliable climatic conclusions for which to reveal the true state of temporal precipitation changes that have occurred in Northeast China.

3.2. Time series analysis method

In order to understand the temporal variation of the precipitation data, the linear trend, climate jumps, and the associated periods, were analyzed by a linear fitted model, the Mann–Kendall test, the moving *t*-test, and the Morlet wavelet method. A linear fitted model is used to test against the null hypothesis slope by means of a two-tailed *t*-test with a confidence level of 95%. It is a common method used for statistical diagnosis in modern climatic analysis studies (Brunetti et al., 2000; Donohue et al., 2010; Liu et al., 2010a; Liang et al., 2010).

The term "climate jump" is also known as "abrupt climate change" and "jump transition" (Li and Li, 1999; Fu and Wang, 1992). It occurs when a climate system is forced to cross certain thresholds, triggering a transition to a new state at a rate determined by the climate itself. The transition will occur at a more rapid rate than the cause that initially set it into motion. This new state will take place so rapidly and unexpectedly that human or natural systems will have difficulty in adapting to it. A change in any measure of climate or variability of climate can be abrupt. This can include a change in the intensity, duration, or frequency of extreme events (Committee on Abrupt Climate Change, National Research Council, 2002). In this study, climate jumps in precipitation in Northeast China were detected by the non-parametric Mann–Kendall test and the moving *t*-test.

3.2.1. Mann–Kendall test

The Mann–Kendall (MK) test (Mann, 1945; Kendall, 1948) has been recommended by the World Meteorological Organization (WMO) in assessing trends in environmental time series data (Yu et al., 2002; Mitchell et al., 1966). The test has been widely used in trend detection analysis for hydrologic and meteorological data (e.g., Hamed, 2008; Liang et al., 2010; Liu et al., 2008). It has the advantage of assuming no special form in relation to the distribution functions of the data. Moreover, subsequences do not have to be setup. An added advantage is that it is nearly as powerful as its parametric competitors.

Time series data points are presumed to be steady, and elements in the series are random and independent from each other. The probability of the element in the series is equal to one another. Under the null hypothesis where no trend is assumed, time series of variables experience no change. The time series could be therefore expressed as $x_1, x_2, \ldots, x_n$. For each term, m_i was computed by the number of terms that occur later in the series and whose values exceed x_i. The MK rank statistic d_k is then specified as:

$$d_k = \sum_{i=1}^{k} m_i \quad (2 \leqslant k \leqslant n) \tag{1}$$

Tied ranks (i.e., repeated ranks) were employed as appropriate fractional contributions to the statistic d_k. Under the null hypothesis where no trend is assumed, the statistic d_k is distributed as a normal (Gaussian) distribution with an expected value of $E(d_k)$ and a variance of $\mathrm{var}(d_k)$ as follows:

$$\begin{aligned} E[d_k] &= k(k-1)/4 \quad (2 \leqslant k \leqslant n) \\ \mathrm{var}[d_k] &= k(k-1)(2k+5)/72 \end{aligned} \tag{2}$$

d_k was standardize as $u(d_k)$ as follows:

$$u(d_k) = (d_k - E[d_k])/\sqrt{\mathrm{var}[d_k]} \quad (2 \leqslant k \leqslant n) \tag{3}$$

The null hypothesis where no trend is assumed will be rejected at a significance level of α if the standard normal probability $prob(|z| > |u(d_k)|) > \alpha$ (Serrano et al., 1999). Given that $u(d_1) = 0$, all $u(d_k)$ will result in a curve C_1. This method was then used to invert the series, that is, for each term, $\overline{m_i}$ was calculated as the number of the former terms in the series whose values exceeded x_i. It follows that:

$$\overline{u}(d_k) = -u(d_{k'}) \quad k' = N + 1 - i \quad (2 \leqslant k \leqslant n) \tag{4}$$

Given that $\overline{u}(d_1) = 0$, all $\overline{u}(d_k)$ will result in a curve C_2. The intersection point of C_1 and C_2 located between the confidence lines was the time that climate jump occurred. A typical confidence level of 95% was used in the detection of the precipitation series.

3.2.2. Moving t-test

The moving t-test (MTT) detects climate jumps in a series by assessing the significant differences between averages of two groups of samples. This method has widely been used in China to detect climate jump events (Fu and Wang, 1992; Lei et al., 2007; Xiang and Chen, 2006; Zhao and Xu, 2006; Li and Jiang, 2007; Liang et al., 2010). When setting a datum point for an n-sample series, the subsequence x_1 of the n_1 samples was obtained before the datum point with an average of $\overline{x_1}$ and a variance of s_1^2, and the subsequence x_2 of the n_2 samples was obtained after the datum point with an average of $\overline{x_2}$ and a variance of s_2^2. The t-statistic is given as (Wei, 1999):

$$t = \frac{\overline{x_1} - \overline{x_2}}{\sqrt{\frac{n_1 s_1^2 + n_2 s_2^2}{n_1 + n_2 - 2}\left(\frac{1}{n_1} + \frac{1}{n_2}\right)}} \tag{5}$$

The null hypothesis that assumes no differences will be rejected if $|t| > t_{\alpha/2}$, given a significance level α. Different length choices of the subsequence set can affect climate jump locations. Two conditions were attempted to combat this: $n_1 = n_2 = 5$ and $n_1 = n_2 = 10$. A typical confidence level of 95% was applied. After calculating the t-statistic, all points satisfying $|t| > t_{\alpha/2}$ constituted the time scope of the climate jump. Climate jumps may appear in years when maximum $|t|$ occurs. $t_{\alpha/2}$ is the t-statistic with a significance level of α (5% for this study).

3.2.3. Morlet wavelet method

Wavelet transforms are a very powerful tool in which to analyze non-stationary signals. It allows for the identification of the main periodicity in a time series and the evolution in time of each frequency. For this study, the complex Morlet wavelet method was used owing to it being the most reliable in detecting variations in geophysical signal periodicity along time scales (Rigozo et al., 2002; Liang et al., 2010). In order to explore the periodicity of precipitation, the application of the Morlet wavelet developed by Torrence and Compo (1998) was closely followed owing to its extensive use among researchers (see Rigozo et al., 2002; EL-Askary et al., 2004; Liang et al., 2010 for application examples). The Matlab wavelet package developed by Torrence and Compo was applied (available online at http://paos.colorado.edu/research/wavelets/).

The Morlet Wavelet is a plane wave modulated by a Gaussian (Torrence and Compo, 1998):

$$\psi_0(\eta) = \pi^{-1/4} e^{i\omega_0\eta} e^{-\eta^2/2} \tag{6}$$

where ω_0 is the non-dimensional frequency taken to be 6 for this study to satisfy the admissibility condition (Farge, 1992).

The wavelet function is expressed as:

$$\hat{\psi}_0(s\omega) = \pi^{-1/4} H(\omega) e^{-(s\omega-\omega_0)^2/2} \tag{7}$$

where s is the wavelet scale; ω is the frequency; and $H(\omega)$ = the Heaviside step function where $H(\omega) = 1$ if $\omega > 0$. $H(\omega) = 0$ otherwise.

3.3. Spatial interpolation method

Numerous algorithms are available to spatially interpolate meteorological data sets such as Inverse Distance Weighted (IDW) and spline as well as various forms of kriging and the trend surface method (Xu et al., 2006; McVicar et al., 2007; Liu et al., 2008; Liang et al., 2010). The trend surface method reflects topographical affects; however, model output from this study in relation to macro geographical factors and precipitation that were established by step regression using Statistical Package for the Social Sciences (SPSS) version 13.0 show that elevation had little effect on precipitation. In light of this, the other four methods were used instead to test for precipitation interpolation in Northeast China. The results are provided in Table 1. Being that the Kriging (exponential) method contains the highest correlation coefficient calculated from the cross-validation test, it was selected for this study to interpolate annual and summer precipitation rates into a 1 km resolution grid for all 98 metrological stations.

4. Results

4.1. Variation of precipitation on a monthly time scale

In order to characterize precipitation on a regional scale, the measurement data taken from the 98 metrological stations were first arithmetically averaged to provide regional values. The regionally averaged time series of the monthly data were then temporally averaged throughout the period from 1961 to 2008 to illustrate dominant patterns in seasonal cycles. Monthly precipitation was highly variable. Fig. 2 shows a strong peak in July in monthly distribution. The peak value was 151 mm month^{-1}, which is considerably higher than values that occurred in preceding months where values did not exceed 10 mm month^{-1}. Summer precipitation (from June to August) accounted for 65.7% of annual precipitation. Standard error was high in months where high precipitation was recorded.

Fig. 3 shows the monthly precipitation trend and its monthly precipitation proportion. The monthly precipitation trend was

Table 1
Comparison of interpolation effectiveness between IDW, spline, Kriging (linear), and Kriging (exponential).

	IDW	Spline	Kriging (linear)	Kriging (spherical)	Kriging (exponential)
Coefficients for annual precipitation	0.962	0.958	0.977	0.941	0.980

Note: values in this table represent the correlation coefficients between the original and modeled values at 15 metrological stations.

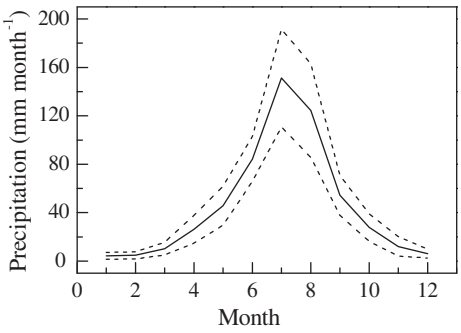

Fig. 2. The monthly precipitation variation averaged between 1961 and 2008 throughout Northeast China. The solid line represents precipitation and the dashed line represents standard error.

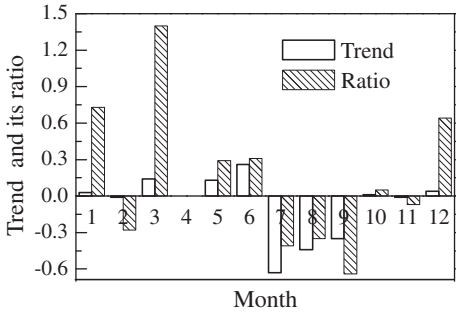

Fig. 3. Trend of monthly precipitation (mm month^{-1} a^{-1}) and its ratio in relation to monthly precipitation (% a^{-1}).

negative in February, July, August, September, and November. The largest trends occurred in July (−0.63 mm month^{-1} a^{-1}) then August (−0.44 mm month^{-1} a^{-1}) and finally September (−0.35 mm month^{-1} a^{-1}). All were negative. The largest positive trend was 0.26 mm month^{-1} a^{-1} that occurred in the month of June. March was the only month to show a significant trend at a 95% confidence level. As far as the ratio between trend and monthly precipitation is concerned, March exhibited the largest precipitation variation with the largest ratio (1.4% a^{-1}), although its trend was not high due to its low monthly precipitation rate.

The ratio of summer precipitation to annual total precipitation averaged in relation to the climatological study period (from 1961 to 2008) for each station was spatially interpolated over Northeast China (Fig. 4). Mean ratios, which reflect the concentration of precipitation to some extent, varied from 53.4% to 75.5% between individual stations. For the most part high ratios were exhibited in regions in the western and middle regions where low precipitation was recorded. These regions include the Songnen Plain and the Greater Khingan Range and are consistent with the results reported by Zhang et al. (2008, 2009).

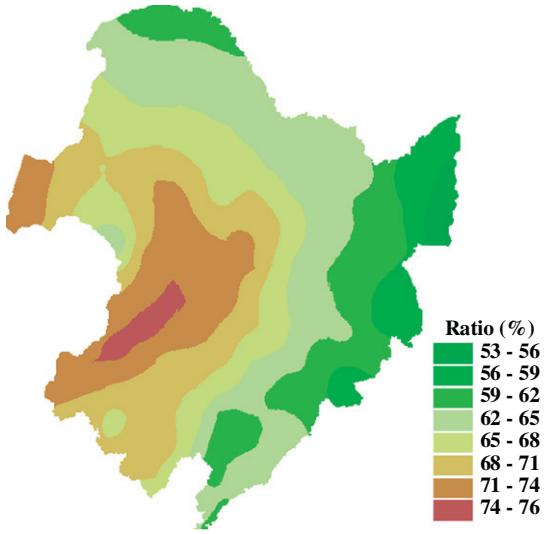

Fig. 4. The spatial distribution of the mean ratios (%) of summer precipitation to annual precipitation between 1961 and 2008 throughout Northeast China.

4.2. Variation of annual and summer precipitation

The spatially averaged annual precipitation rate in Northeast China from 1961 to 2008 was 503 mm a^{2}, varying throughout the 48 years with a range that fluctuated between 435 and 680 mm a^{-1} and a variation coefficient of 0.11. The highest annual precipitation rate was approximately 1.56 times that of the lowest value. Summer precipitation with a spatial average of 333 mm season^{-1}, accounting for 65.7% of the total annual value, reflected the variation in total annual precipitation (Fig. 5). The cumulative precipitation anomaly substantiated this measurement (Fig. 6). Both annual and summer precipitation rates decreased during the study period exhibiting a trend of −0.82 mm a^{-2} and −0.81 mm season^{-1} a^{-1}, respectively. The ratio of summer precipitation to annual precipitation remained virtually unchanged, exhibiting only an insignificant variation of −0.061% a^{-1} from 1961 to 2008.

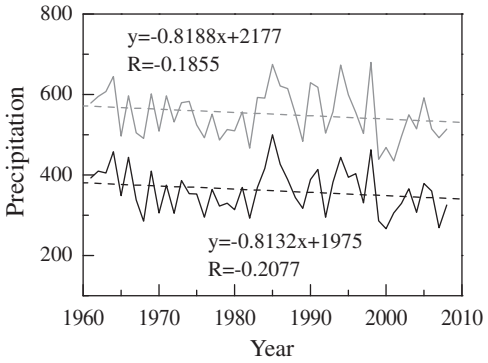

Fig. 5. Temporal variation of precipitation between 1961 and 2008 throughout Northeast China. The light gray curve and dashed line represent annual precipitation (mm a^{-1}) and its corresponding trend line. The black curve and dashed line represent summer precipitation (mm season^{-1}) and its corresponding trend line.

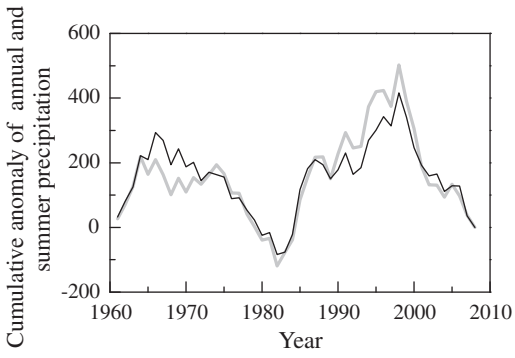

Fig. 6. Cumulative anomaly of annual (light gray, in mm a^{-1}) and summer (black in mm season^{-1}) precipitation between 1961 and 2008 throughout Northeast China.

The trends for the two series are almost identical. This is a result of the decrease in precipitation that primarily occurred in summer. Precipitation for both series can be divided into three periods where lower values occurred from 1961 to 1982, higher values occurred from 1983 to 1998, and lower values reoccurred from 1999 to 2008. For annual precipitation the averages were 546, 590, and 502 mm a^{-1} for the three periods, respectively, while for summer precipitation the averages were 356, 392, and 319 mm $season^{-1}$ for the three periods, respectively. During the last 8 years (except for 1981 where values were somewhat higher than the averages) of the first period, annual and summer precipitation rates were lower than the 48 year average. After the floods that took place in 1998, annual precipitation rates for the following 6 years were once again all lower than the 48 year average.

4.3. Spatial distribution of precipitation trends

Trends that occurred at individual stations were calculated in order to reflect temporal trends for different regions. Fig. 7 shows the spatial distribution of trends for annual and summer precipitation. Annual precipitation decreased at 77 of the 98 metrological stations. The decreasing trend was higher on the peninsula in the southern study area within Northeast China, the plains of the Liao River, the southern region of the Songnen Plain as well as Lesser Khingan Range located in the northern study area. The highest decreasing trend was measured at the Xiongyue metrological station in the plains of the Liao River (-3.86 mm a^{-2}). The highest increasing trend was measured at the Hulin metrological station in the Sanjiang Plain (1.35 mm a^{-2}). Increasing precipitation trends distributing to the north of lat 42°N was detected. The decreasing precipitation trend for the following four stations was significant at a 5% significance level. The four stations are the Tongyu metrological station located on the Songnen Plain, the Changbai metrological station located in the Changbai Mountains, and the Xiongyue and Xiuyan metrological stations located on the peninsula. While increasing precipitation trends for all stations were insignificant, it can be concluded that the southern study area contributed more to the decreasing trend in terms of precipitation in relation to Northeast China as a whole (see Fig. 5).

Similar to the annual series, summer precipitation decreased at 80 of the 98 metrological stations. No significant change was found in increasing trends. The range of trends for summer precipitation was between -3.7 and 1.5 mm $season^{-1}$ a^{-1}. However, five other stations (one located on the Sanjiang Plain, two located on Lesser Khingan Range, and two located along the coastline of the peninsula) measured significant decreasing trends for the summer precipitation series with the exception of the four stations where significant trends were detected for the annual series. It is clear that precipitation decreased in most areas of Northeast China throughout the 1961–2008 period under investigation, and that the change in annual precipitation was primarily attributed to the change in summer precipitation. This conclusion supports previous results that conclude that annual variation in summer precipitation reflected the annual variation in precipitation.

4.4. Annual and summer precipitation climate jumps

MK results on precipitation throughout the 1961–2008 investigative period in Northeast China showed that the climate jumps which occurred in both the annual and summer series parallel each other (Fig. 8). For both series, three climate jumps took place in 1967, 1983, and 1998, showing decreasing, increasing, and decreasing precipitation changes, respectively. Moreover, these results are confirmed by the cumulative precipitation anomaly curve provided in Fig. 6.

Fig. 9 provides the MTT results with regards to annual and summer precipitation throughout the 1961 to 2008 investigative period in Northeast China. Three climate jumps took place in 1975, between 1982 and 1983, and 1998 for the annual series and in 1966, between 1982 and 1983, and 1998 for the summer series when the two subsequences were both 5 years long. When the two subsequences were both 10 years long, two climate jumps took place between 1981 and 1984 and in 1998 for both the annual and summer series. It appears that climate jump occurrences are sensitive to the choice of the length of the subsequences. According to the location of the maximum absolute t-statistic, climate jumps were found to occur in the annual series in 1975 ($n_1 = n_2 = 5$), 1982 ($n_1 = n_2 = 5$ and $n_1 = n_2 = 10$), and 1998 ($n_1 = n_2 = 5$ and $n_1 = n_2 = 10$), and climate jumps were found to occur in the summer series in 1966 ($n_1 = n_2 = 5$), 1982 ($n_1 = n_2 = 5$ and $n_1 = n_2 = 10$), and 1998 ($n_1 = n_2 = 5$ and $n_1 = n_2 = 10$). It is clear that subsequences with more than one length are necessary in climate jump detection

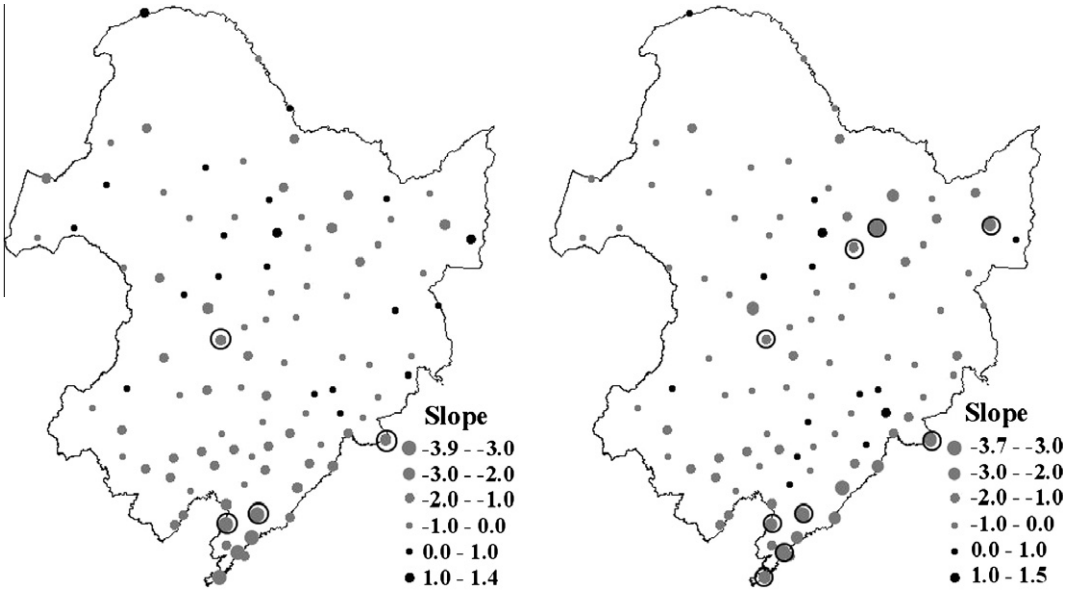

Fig. 7. Trends in annual (a, in mm a^{-2}) and summer (b, in mm $season^{-1}$ a^{-1}) precipitation between 1961 and 2008 in Northeast China. A ring was placed around the circle if the trend was significant at a 95% confidence level.

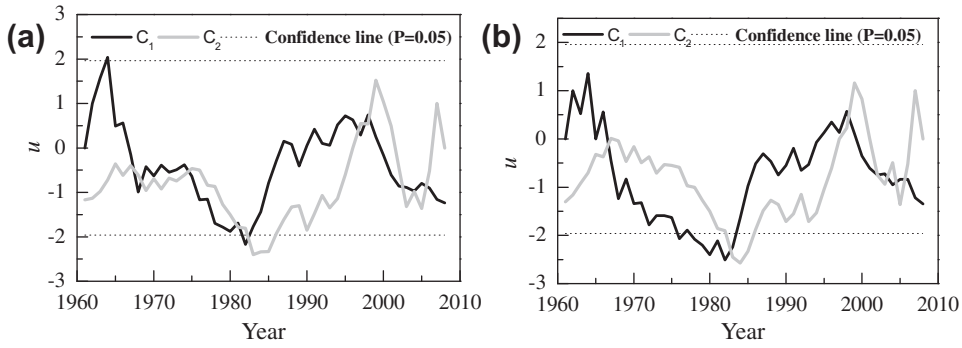

Fig. 8. Mann–Kendall analyses of annual (a) and summer (b) precipitation between 1961 and 2008 throughout Northeast China. Since line C_1 extended the confidence line ($P = 0.05$), the cross point of C_1 and C_2 was the start point of a climate jump in this series.

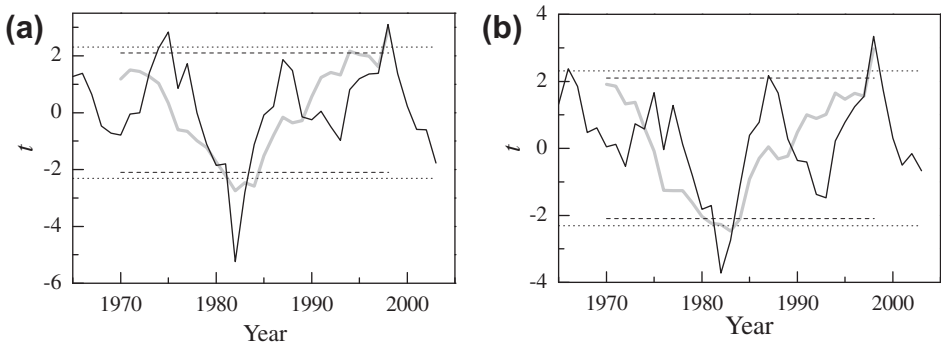

Fig. 9. Moving t-test for annual (a) and summer (b) precipitation between 1961 and 2008 throughout Northeast China. Dark and light gray lines represent the statistics when $n_1 = n_2 = 5$ and $n_1 = n_2 = 10$, respectively; dot and dashed lines represent a significance level of 0.05 when $n_1 = n_2 = 5$ and $n_1 = n_2 = 10$, respectively.

since they assess significant differences between the averages of two groups of samples.

Since climate jumps detected by the MK method reflect a significant change in trends and climate jumps detected by the MTT method indicate a significant difference between the averages of the two subsequence series, results provided by the two methods are not necessarily consistent (Hao, 2003; Liang et al., 2010). What is certain is that times when climate jumps occurred in the different precipitation series paralleled each other, and both methods applied were in agreement with this result. Results for both precipitation series were consistent with the MK method. Similarly, results for both methods were also consistent with the summer series. Therefore, a point to be noted is that the climate jump detected by MTT in the annual series that occurred in 1975 was different from the other three climate jumps that first occurred in 1966 or 1967. The timing of the second and third climate jump events was consistent in both series by both methods applied. At least to some extent the two methods (MK and MTT) can be used to supplement and verify each other in the detection of climate jump phenomena.

4.5. Periodicity of annual and summer precipitation

The annual and summer precipitation series were detected by means of Morlet wavelet transforms in order to investigate precipitation periodicity. Period detection results of annual precipitation in Northeast China are provided in Fig. 10. The mean of the entire record was removed to define an anomaly time series. Annual precipitation anomaly is provided in Fig. 10a. From variations in frequency of occurrence and amplitudes of precipitation events illustrated in Fig. 10b, it can be deduced that numerous dry and humid events occurred between 1961 and 1975 and between 1985 and 2002. However, few of these events occurred between 1975 and 1985. Between 1960 and 1975 there is a shift from shorter to longer periods while between 1985 and 2002 the shift alters from slightly longer to slightly shorter periods. During the 1960s and the period between 1985 and 2002 the variance in the 2–8 year band is significantly above the 95% confidence level (Fig. 10d). For annual precipitation, there were periods of 2.5 and 3.5 years which were both significant at a 95% confidence level (Fig. 10b and c). Another period that persisted for 9 years was not significant. It must therefore be determined that significant periods of precipitation are short. Summer precipitation periodicity was consistent with that of annual precipitation, since summer precipitation accounted for a high percentage of annual precipitation. While, variance that occurred in the 1960s for the summer series was higher than that which occurred for the annual series. The 2–4 year period was linked with El Niño events. Precipitation was lower than normal in the year El Niño events occurred and continued into the following year.

5. Discussion

5.1. Influence of temporal precipitation variation on agriculture and ecosystems

Spring drought and summer waterlogging are highly susceptible to monthly scale precipitation patterns and have a significant effect on agriculture and ecosystem water requirements (Liu, 2001), especially in rain-fed agricultural regions such as certain areas within the Songnen Plain and the plains of the Liao River. Precipitation patterns contribute to the reduction of agriculture production, causing more difficulties in the planning and management of agricultural production in these regions. Furthermore, high

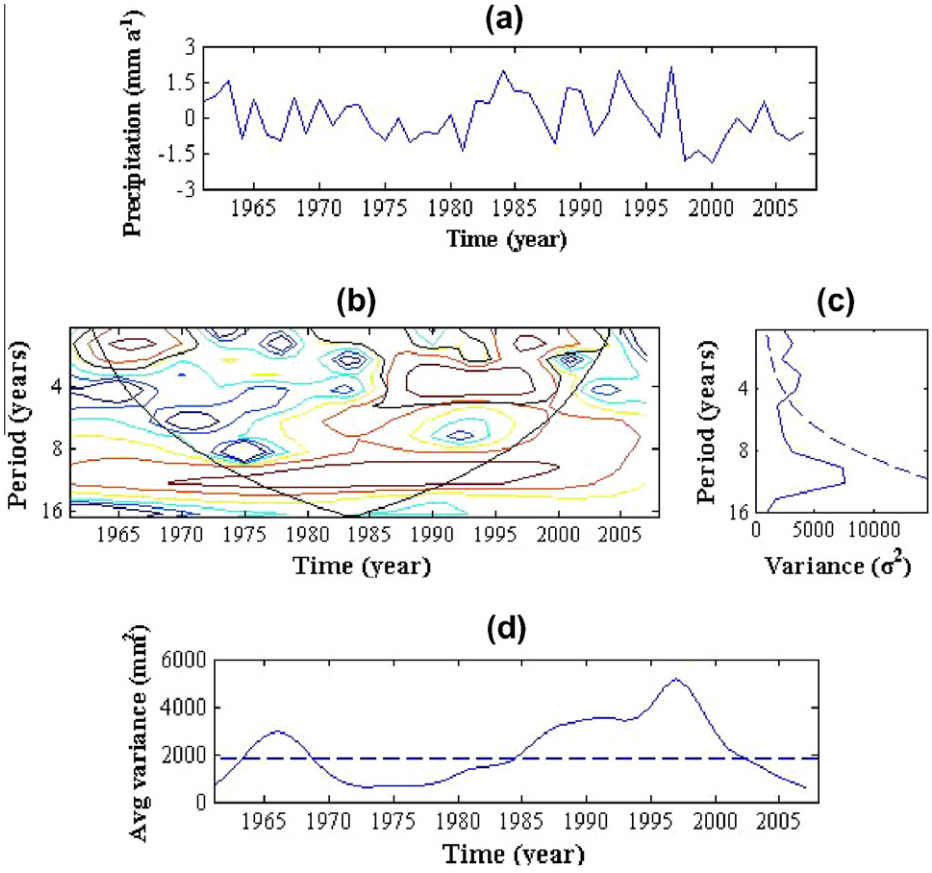

Fig. 10. Morlet wavelet transformation of annual precipitation anomaly between 1961 and 2008 throughout Northeast China. (a) is the annual precipitation time series used for wavelet analysis and (b) is the local wavelet power spectrum of (a). The thick black contour line designates a 5% significance level against any red noise, and the cone of influence (COI) where edge effects may distort the picture is shown under a thin black curve. (c) is the Fourier power spectrum of the annual precipitation (solid line). The dashed line represents the 95% confidence spectrum. (d) is the scale-averaged wavelet power throughout the 2–8 year band for annual precipitation (solid line). The dashed line represents a 95% confidence level.

concentration along with low precipitation is ultimately unfavorable to forest conservation. Incidences of forest fire, such as the great forest fire that took place in the Greater Khingan Range in the summer of 2010, may increase (Li, 2010).

A report published by IPCC (2007) stated that precipitation has increased throughout the twentieth century between latitude 30°N and 85°N. This is inconsistent with the findings of this study where a decreasing trend was ascertained in relation to precipitation in Northeast China between 1961 and 2008. Moreover, this decreasing trend in annual precipitation is extremely high compared to other areas in China as well as other countries throughout the world (Table 2). The trend exhibited in the Liao River catchment was similar to that in this study. However, the trend in the Songhua River catchment was much less than that measured in Northeast China, which may be the result of conflicting data sets from different stations and the period length applied in the statistics used. WMO defined climatological standard normals as "averages of climatological data computed for the following consecutive 30 year periods: from January 1, 1901, to December 31, 1930, from January 1, 1931, to December 31, 1960, etc." (WMO, 1984). The latest official period of recognized global standard climate normals is the period from 1961 to 1990. Compared to WMO climate normals from 1961 to 1990, mean annual precipitation in the last decade (502 mm a^{-1}) decreased by 10.3%. Water resources become scarce during times of lower precipitation (i.e., that which occurred from 1999 to 2008) due to interannual variation. The result is that ecological water requirements of wetlands can barely be met in some instances, for example, the Zhalong wetland and the Xianghai wetland. For 13 years, between 1990 and 2005, discontinuous flow was recorded in the Taoer River. No streamflow was recorded in Taonan, the control station of the middle reaches, in 2002, 2003, and 2004 (Liang, 2008). In order to maintain wetland health, water allocation initiatives have been implemented by local governments. Between 2001 and 2007, 1.1 billion m^3 of water was imported to the Zhalong wetland in five separate stages. Furthermore, water scarcity, resulting from decreasing trends in precipitation, also has a negative effect on the implementation of the "Plan for Increasing the National Grain Production Capacity by 50 Billion Kilograms (2009–2020)." All these factors suggest that more suitable strategies must be implemented to meet the water requirements of agriculture and natural ecosystems in Northeast China.

5.2. Influence of spatial distribution of precipitation on agriculture and ecosystems

Precipitation showed large spatial variation in Northeast China due to the East Asian monsoon and to topography (Fig. 11). Mean annual precipitation varied between 243 and 1073 mm a^{-1} at individual metrological stations, and mean summer precipitation varied from 182 to 703 mm $season^{-1}$. Precipitation for both the annual and summer series decreased in a southeastern to a northwestern trajectory with high values measured in the Changbai Mountains. Precipitation in Lesser Khingan Range was higher

Table 2
Precipitation trends as reported by other researches.

Area	Country	Period	Precipitation (mm a^{-1})	Change (%)	Trend (mm a^{-2})	References
Pear River (Zhujiang) catchment	China, Asia	1951–2000	1469	2	i.e. 0.59	Xu et al. (2010)
Yangtze River (Changjiang) catchment	China, Asia	1951–2000	1045	−1	i.e. −0.21	Xu et al. (2010)
Yellow River (Huanghe) catchment	China, Asia	1951–2000	442	−11	i.e. −0.97	Xu et al. (2010)
Liao River catchment	China, Asia	1951–2000	505	−8	i.e. −0.81	Xu et al. (2010)
Songhua River catchment	China, Asia	1951–2000	521	−4	i.e. −0.42	Xu et al. (2010)
Hengduan Mountains (in the southeastern part of Tibet	China, Asia	1960–2008			0.91	Li et al. (2010)
China	China, Asia	1951–2000			0.14	Liu et al. (2010b)
Korea	Korea, Asia	1961–2007			6.7	Yum and Cha (2010)
Kerala	India, Asia	1871–2005			−0.54	Krishnakumar et al. (2009)
Botswana	Botswana, Africa	1975–2005			−1.38	Batisani and Yarnal (2010)
French Mediterranean region	France, Europe	1971–2006			0	Chaouche et al. (2010)
North Italy	Italy, Europe	1867–1995			−0.47	Brunetti et al. (2000)
South Italy	Italy, Europe	1867–1995			−1.04	Brunetti et al. (2000)

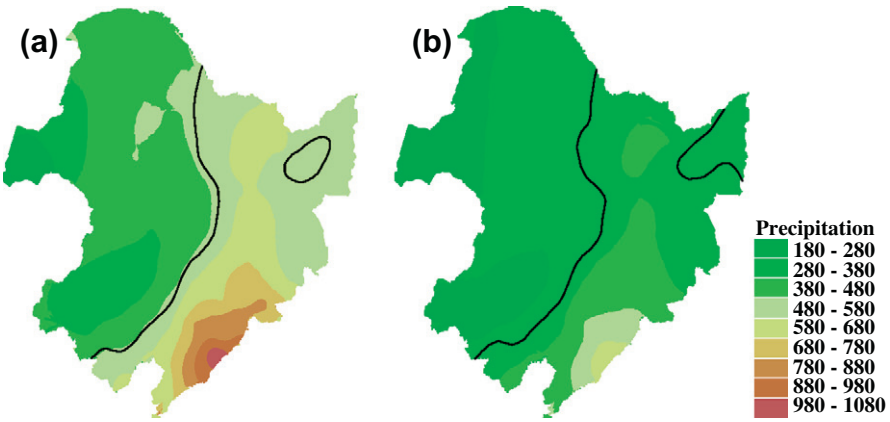

Fig. 11. The spatial distribution of mean annual (a, in mm a^{-1}) and summer precipitation (b, in mm $season^{-1}$) between 1961 and 2008 in Northeast China. Black lines represent 500 mm a^{-1} and 330 mm $season^{-1}$ for annual and summer precipitation, respectively.

owing to topographical factors. The magnitude of summer precipitation was less than the magnitude of annual precipitation, especially in the southern region where there exists a lower summer to annual precipitation ratio. Northeast China can be divided into the eastern zone with higher precipitation and the western zone with lower precipitation, according to the corresponding mean precipitation line (500 mm a^{-1} in Fig. 11a and 330 mm $season^{-1}$ in Fig. 11b). The sole exception was an area within the Sanjiang Plain.

Spatial variation in precipitation led to a greater amount of rain occurring in the eastern zone and a lesser amount of rain occurring in the western zone. This resulted in floods (e.g., the floods that took place in the Second Songhua River basin in the summer of 2010) and water shortages (that impacted important wetland nature reserves and agricultural areas). Yang et al. (2008) reported that the extreme precipitation (higher than the average daily precipitation at the 99th percentile in a given year between 1961 and 1990) increased in frequency, especially in the lower reaches of the Songhua River basin, Mudan River basin, and the upper reaches of the West Liao River basin. According to the research carried out by Sun et al. (2006), dry spells greater than 10 days in duration occurred mostly in the western and middle plains region between 1951 and 2002, and exhibited an increasing trend in frequency. The low precipitation rate taking place in the Songnen Plain (with a mean value of 468 mm a^{-1} or 326 mm $season^{-1}$ during the summer), which is the most important factor that restricts agricultural development, has become the biggest obstacle in increasing the capacity of grain production.

5.3. Response of precipitation variation to climate change

The spatial distribution of climate jumps in precipitation suggests that most regions in Northeast China are highly sensitive to climate change. For the annual series (Fig. 12a), one climate jump took place at 44 metrological stations, two at 18, and three at 13. No climate jumps were detected at 23 metrological stations for this series. For the summer series (Fig. 12b), one climate jump took place at 31 metrological stations, two at 22, and three at 13. No climate jumps were detected at 32 metrological stations for this series. The metrological stations for which climate jumps were detected totaled 77% (75 of 98) for the annual series and 67% (66 of 98) for the summer series. The number of metrological stations where two or three climate jumps were detected was almost the same for both the annual and the summer series. However, a greater number of climate jumps occurred in the annual series than in the summer series for metrological stations where only one climate jump was detected. This was mainly owing to metrological stations located in the Changbai Mountains and the peninsula that only exhibited climate jumps in the annual series. Although the numbers of metrological stations that showed the same number of climate jumps were similar for both precipitation series, the specific stations were different.

For both the annual and the summer precipitation series, metrological stations where three climate jumps were detected exhibited a decreasing, increasing, and decreasing change in sequence, and those with two climate jumps exhibited one decreasing and one increasing change. As far as the series where only one

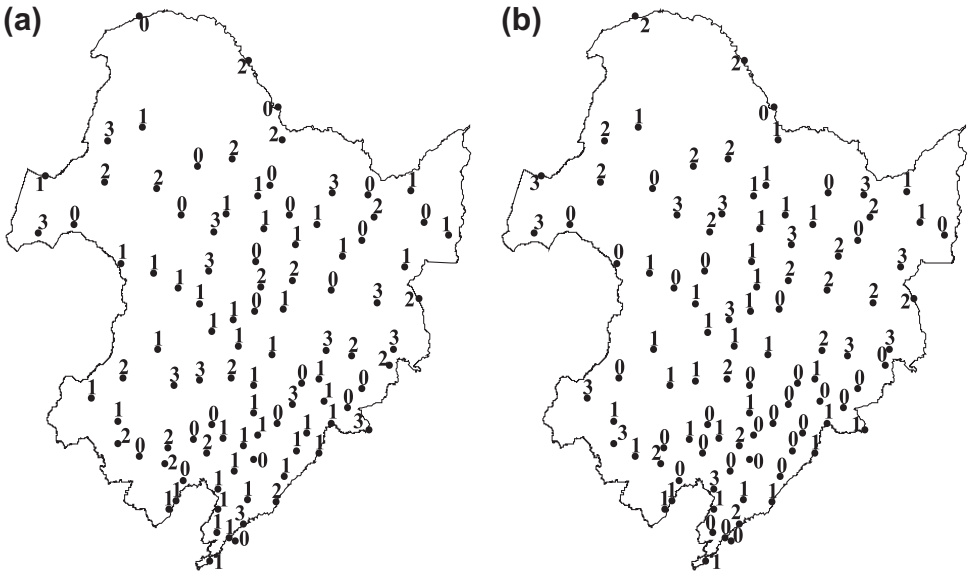

Fig. 12. Distribution of times of climate jumps for annual (a) and summer (b) precipitation between 1961 and 2008 throughout Northeast China. Dots represent meteorological stations and numbers represent times of climate jumps.

climate jump occurred is concerned, all metrological stations exhibited a decreasing trend except for four that showed an increasing trend for both the annual series and the summer series. Three of the four metrological stations were the same for both the annual and the summer series, and the timings of all upward climate jumps occurred in the middle period of the entire study period. Downward trends, revealed by way of climate jumps, also explain decreasing trends in precipitation, which is consistent with the results obtained by the linear fitted model.

6. Conclusions

Precipitation, being one of the most important variables in diagnosing climate change, can be utilized to reveal eco-hydrological processes of climate change on a regional scale. For this study, spatial and temporal variations in precipitation were analyzed by a linear fitted model, the Mann–Kendall test, the moving *t*-test, and the Morlet wavelet and Kriging (exponential) interpolation methods in Northeast China. Their influence on ecosystems and agriculture and their response to climate change were discussed. Three main conclusions may be drawn:

(a) Monthly precipitation showed high concentrations in relation to summer precipitation that accounted for 65.7% of the annual total value, which can result in spring drought and summer waterlogging events and influence the overall health of agriculture and ecosystems in the region.

(b) Precipitation for Northeast China as a whole decreased between 1961 and 2008 with a trend measured at -0.82 mm a^{-2} for the annual series and -0.81 mm season^{-1} a^{-1} for the summer series. This was validated by the decreasing trend observed at most of the 98 metrological stations investigated. Annual precipitation in the last 10 years was 10.3% lower than WMO climate normals between 1961 and 1990.

(c) Three climate jumps were tested on a regional scale in 1967 (MK)/1975 (MTT), between 1982 (both MK and MTT), and 1998 (both MK and MTT). These revealed a decreasing, increasing, and a decreasing trend in precipitation, respectively. Moreover, climate jumps occurred at most stations one, two, or three times. Periods of 2.3 and 3.3 years (significant at a 95% confidence level) were detected for both annual and summer precipitation rates on a regional scale. They are linked to El Niño events. Precipitation was lower than normal in the year El Niño events occurred and continued into the following year.

(d) Northeast China experienced high levels of variability in precipitation, decreasing in a southeastern to northwestern trajectory due to the influence of the East Asian monsoon and to topography. The spatial distribution of precipitation led to water shortages for ecological conservation and agricultural development in the western and middle regions, especially in the Songnen Plain, an important agricultural region as stated by the "Plan for Increasing the National Grain Production Capacity by 50 Billion Kilograms (2009–2020)."

Acknowledgments

This research was supported by the Key Project of Knowledge Innovation Program (CAS) (Project No. KZCX2-YW-Q06-1) and the Chinese Postdoctoral Science Foundation (Project No. 20090450562).

References

Abdul Aziz, O.I., Burn, D.H., 2006. Trends and variability in the hydrological regime of the Mackenzie River Basin. J. Hydrol. 319, 282–294.

Batisani, N., Yarnal, B., 2010. Rainfall variability and trends in semi-arid Botswana: implications for climate change adaptation policy. Appl. Geogr. 30, 483–489.

Brunetti, M., Maugeri, M., Nanni, T., 2000. Variations of temperature and precipitation in Italy from 1866 to 1995. Theor. Appl. Climatol. 65, 165–174.

Cannarozzo, M., Noto, L.V., Viola, F., 2006. Spatial distribution of rainfall trends in Sicily (1921–2000). Phys. Chem. Earth 31, 1201–1211.

Chaouche, K., Neppel, L., Dieulin, C., Pujol, N., Ladouche, B., Martin, E., Salas, D., Caballero, Y., 2010. Analyses of precipitation, temperature and evapotranspiration in a French Mediterranean region in the context of climate change. CR Geosci. 342, 234–243.

Committee on Abrupt Climate Change, National Research Council, 2002. "Definition of Abrupt Climate Change". Abrupt Climate Change: Inevitable Surprises. National Academy Press, Washington, DC. <http://www.nap.edu/catalog/10136.html>.

Donohue, R.J., McVicar, T.R., Roderick, M.L., 2010. Assessing the ability of potential evaporation formulations to capture the dynamics in evaporative demand within a changing climate. J. Hydrol. 386, 186–197.

EL-Askary, H., Sarkar, S., Chiu, L., Kafatos, M., El-Gahzawi, T., 2004. Rain gauge derived precipitation variability over Virginia and its relation with the El Nino southern oscillation. Adv. Space Res. 33, 338–342.
Farge, M., 1992. Wavelet transforms and their applications to turbulence. Annu. Rev. Fluid Mech. 24, 395–457.
Fu, C.B., Wang, Q., 1992. The definition and detection of the abrupt climate change. Sci. Atmos. Sin. 16 (4), 482–493 (in Chinese with English abstract).
Guo, R., Wang, X.K., Ouyang, Z.Y., Li, Y.N., 2006. Spatial and temporal relationships between precipitation and ANPP of four types of grasslands in northern China. J. Environ. Sci. 18 (5), 1024–1030.
Hamed, K.H., 2008. Trend detection in hydrologic data: the Mann–Kendall trend test under the scaling hypothesis. J. Hydrol. 349, 350–363.
Hao, Z.X., 2003. Reconstruction and Analysis of Precipitation Series for the last 300 years over the Middle and Lower Reaches of the Yellow River. PhD Thesis. Graduate University of Chinese Academy of Sciences, Beijing, 122 (in Chinese with English abstract).
IPCC, 1995. In: Houghton, J.T., Meira Filho, L.G., Callander, B.A., Harris, N., Kattenberg, A., Maskell, K. (Eds.), Climate Change 1995: Radiative Forcing of Climate Change and An Evaluation of the IPCC IS92 Emission Scenarios. Cambridge Univ. Press, Cambridge, UK.
IPCC, 2007. In: Pachauri, R.K., Reisinger, A. (Eds.), Climate Change 2007: Synthesis Report. Contribution of Working Groups I, II and III to the Fourth Assessment Report of the Intergovernmental Panel on Climate Change. IPCC, Geneva, Switzerland, 104 pp.
Jiang, D.J., Li, L.J., Hou, X.Y., Liang, L.Q., Zhang, L., Li, J.Y., Xu, M.X., 2009. Variations in the hydrological cycle components and their influencing factors in the middle and upper reaches of Tao'erhe River Basin. Geogr. Res. 28 (1), 55–64.
Kendall, M.G., 1948. Rank Correlation Methods. Hafner, New York.
Krishnakumar, K.N., Prasada Rao, G.S.L.H.V., Gopakumar, C.S., 2009. Rainfall trends in twentieth century over Kerala, India. Atmos. Environ. 43, 1940–1944.
Lei, H.F., Xie, P., Chen, G.C., Li, J., 2007. Comparison and analysis on the performance of hydrological time series change-point testing methods. Water Resour. Power 25 (4), 36–40 (in Chinese with English abstract).
Li, C.Y., Li, G.L., 1999. Variation of the NAO and NPO associated with climate jump in the 1960s. Chin. Sci. Bull. 44 (21), 1983–1987. doi:10.1007/BF02887124.
Li, P., 2010. Causes for fire in the Greater Khingan Mountains. Beijing Science and Technology News. <http://bkb.ynet.com/article.jsp?oid=67350219>.
Li, Z., Jiang, F.Q., 2007. A Study of abrupt climate change in Xinjiang region during 1961–2004. J. Glaciol. Geocryol. 29 (3), 351–359 (in Chinese with English abstract).
Li, Z.X., He, Y.Q., Wang, C.F., Wang, X.F., Xin, H.J., Zhang, W., Cao, W.H., 2010. Spatial and temporal trends of temperature and precipitation during 1960–2008 at the Hengduan Mountains, China. Quatern. Int. xxx, 1–16.
Liang, L.Q., 2008. Spatial-Temporal Pattern and Evolution Mechanism of Evapotranspiration in the Taoer River basin. Ph.D. Dissertation. Graduate University of Chinese Academy of Sciences, Beijing, 38 (in Chinese with English abstract).
Liang, L.Q., Li, L.J., Liu, Q., 2010. Temporal variation of reference evapotranspiration during 1961–2005 in the Taoer River basin of Northeast China. Agric. Forest Meteorol. 150, 298–306.
Liu, C.M., 2007. Research on Water and Ecological–Environmental Problems and The Countermeasures. Science Press, Beijing, China.
Liu, Q., Yang, Z.F., Cui, B.S., 2008. Spatial and temporal variability of annual precipitation during 1961–2006 in Yellow River Basin, China. J. Hydrol. 361, 330–338.
Liu, Q., Yang, Z.F., Cui, B.S., Sun, T., 2010a. The temporal trends of reference evapotranspiration and its sensitivity to key meteorological variables in the Yellow River Basin, China. Hydrol. Process.. doi:10.1002/hyp.7649.
Liu, X.T. (Ed.), 2001. Management on Degraded Land and Agricultural Development in the Songnen Plain. Science Press, Beijing, p. P12-13 (in Chinese).
Liu, Y.X., Li, X., Zhang, Q., Guo, Y.F., Gao, G., Wang, J.P., 2010b. Simulation of regional temperature and precipitation in the past 50 years and the next 30 years over China. Quatern. Int. 212, 57–63.
Mann, H.B., 1945. Non-parametric test against trend. Econometrika 13, 245–259.
McVicar, T.R., Van Niel, T.G., Li, L.T., Hutchinson, M.F., Mu, X.M., Liu, Z.H., 2007. Spatially distributing monthly reference evapotranspiration and pan evaporation considering topographic influences. J. Hydrol. 338, 196–220.
Mitchell, J.M., Dzerdzeevskii, B., Flohn, H., Hofmeyr, W.L., Lamb, H.H., Rao, K.N., Wallén, C.C., 1966. Climatic Change, WMO Technical Note No. 79. World Meteorological Organization, 79.
Ni, J., Zhang, X.S., 2000. Climate variability, ecological gradient and the Northeast China Transect (NECT). J. Arid Environ. 46, 313–325.
O'Neal, M.R., Frankenberger, J.R., Ess, D.R., 2002. Use of CERES-Maize to study effect of spatial precipitation variability on yield. Agric. Syst. 73, 205–225.
Oguntunde, P.G., Friesen, J., van de Giesen, N., Savenije, H.H.G., 2006. Hydroclimatology of Volta River Basin in West Africa: trends and variability from 1901 to 2002. Phys. Chem. Earth 31, 1180–1188.
Rigozo, N.R., Nordemann, D.J.R., Echer, E., Zanandrea, A., Gonzalez, W.D., 2002. Solar variability effects studied by tree-ring data wavelet analysis. Adv. Space Res. 29 (12), 1985–1988.
Serrano, A., Mateos, V.L., Garcia, J.A., 1999. Trend analysis of monthly precipitation over the Iberian Peninsula for the period 1921–1995. Phys. Chem. Earth 24, 85–90.
Sun, F.H., Wu, Z.J., Yang, S.Y., 2006. Temporal and spatial variations of extreme precipitation and dryness events in Northeast China in last 50 years. Chin. J. Ecol. 25 (7), 779–784 (in Chinese with English abstract).
Torrence, C., Compo, G.P., 1998. A practical guide to wavelet analysis. Bull. Am. Meteorol. Soc. 79, 61–78.
Wei, F.Y., 1999. Statistical Techniques of Modern Climatic Diagnosis and Forecasting. China Meteorological Press, Beijing, pp. 63–65 (in Chinese).
Wei, H., Li, J.L., Liang, T.G., 2005. Study on the estimation of precipitation resources for rainwater harvesting agriculture in semi-arid land of China. Agric. Water Manage. 71, 33–45.
Westmacott, J.R., Burn, D.H., 1997. Climate change effects on the hydrologic regime within the Churchill–Nelson River Basin. J. Hydrol. 202 (1), 263–279.
WMO, 1984. Technical Regulations, vol. I. WMO Publication No. 49. Geneva, Switzerland.
Xiang, L.Y., Chen, X., 2006. Regional and seasonal features of abrupt temperature Change in China in recent 55 years. Meteorol. Month. 32 (6), 44–47 (in Chinese with English abstract).
Xu, C.Y., Gong, L.B., Jiang, T., Chen, D.L., Singh, V.P., 2006. Analysis of spatial distribution and temporal trend of reference evapotranspiration and pan evaporation in Changjiang (Yangtze River) catchment. J. Hydrol. 327, 81–93.
Xu, K.H., Milliman, J.D., Xu, H., 2010. Temporal trend of precipitation and runoff in major Chinese Rivers since 1951. Global Planet. Change, 73 219–232.
Yang, S.Y., Sun, F.H., Ma, J.Z., 2008. Evolvement of precipitation extremes in northeast china on the background of climate warming. Chin. Geogr. Sci. 28 (2), 224–228 (in Chinese with English abstract).
Yin, P.H., Fang, X.Q., Tian, Q., Ma, Y.L., 2006. Distribution and regional difference of main output regions in grain production in China in the early 21st century. Acta Geogr. Sin. 61 (2), 190–198 (in Chinese with English abstract).
Yu, P.S., Yang, T.C., Wu, C.K., 2002. Impact of climate change on water resources in southern Taiwan. J. Hydrol. 260, 161–175.
Yum, S.S., Cha, J.W., 2010. Suppression of very low intensity precipitation in Korea. Atmos. Res. 98, 118–124.
Zhang, Y.F., Hu, C.L., Zhao, C.Y., Wang, Y., Ren, G.Y., 2009. Intra-annual inhomogeneity characteristics of precipitation in Northeast China. J. Natural Disasters 18 (2), 89–94.
Zhang, S.W., Zhang, Y.Z., Li, Y., Chang, L.P., 2006. Temporal and Spatial Variations of Land Use/Cover Changes in Northeast China. Sciences Press, Beijing, China (in Chinese).
Zhang, W., Zhang, T.Y., Liu, J., 2008. Temporal and spatial features of precipitation-concentration degree and precipitation-concentration period of annual rainfall over Northeast China. J. Nanjing Inst. Meteorol. 31 (3), 403–410 (in Chinese with English abstract).
Zhao, F.F., Xu, Z.X., 2006. Long term trend and jump change for major climate processes over the upper Yellow River Basin. Acta Meteorol. Sin. 64 (2), 246–255 (in Chinese with English abstract).